Fracturing and fluid-flow during post-rift subsidence in carbonates of the Jandaíra Formation, Potiguar Basin, NE Brazil

Bertotti, Giovanni; de Graaf, Stefan; Bisdom, Kevin; Oskam, Brigit; B. Vonhof, Hubert; H. R. Bezerra, Francisco; J. G. Reijmer, John; L. Cazarin, Caroline

DOI
10.1111/bre.12246

Publication date
2017

Document Version
Final published version

Published in
Basin Research

Citation (APA)
Bertotti, G., de Graaf, S., Bisdom, K., Oskam, B., B. Vonhof, H., H. R. Bezerra, F., J. G. Reijmer, J., & L. Cazarin, C. (2017). Fracturing and fluid-flow during post-rift subsidence in carbonates of the Jandaíra Formation, Potiguar Basin, NE Brazil. *Basin Research*, *29*(6), 836–853. https://doi.org/10.1111/bre.12246

Basin Research

IAS EAGE

Basin Research (2017) 1–18, doi: 10.1111/bre.12246

Fracturing and fluid-flow during post-rift subsidence in carbonates of the Jandaíra Formation, Potiguar Basin, NE Brazil

Giovanni Bertotti,* Stefan de Graaf,†,1 Kevin Bisdom,* Brigit Oskam,† Hubert B. Vonhof,‡ Francisco H. R. Bezerra,§ John J. G. Reijmer†,1 and Caroline L. Cazarin¶

*Department of Geoscience and Engineering, Delft University of Technology, Delft, the Netherlands
†Department of Earth Sciences, VU University Amsterdam, Amsterdam, the Netherlands
‡Max Planck Institute of Chemistry, Mainz, Germany
§Department of Earth Sciences, Federal University Rio Grande do Norte, Rio Grande do Norte, Brazil
¶CENPES, Petrobras R&D Center, Rio de Janeiro, Brazil

ABSTRACT

Pervasive fracture networks are common in many reservoir-scale carbonate bodies even in the absence of large deformation and exert a major impact on their mechanical and flow behaviour. The Upper Cretaceous Jandaíra Formation is a few hundred meters thick succession of shallow water carbonates deposited during the early post-rift stage of the Potiguar rift (NE Brazil). The Jandaíra Formation in the present onshore domain experienced <1.5 km thermal subsidence and, following Tertiary exhumation, forms outcrops over an area of >1000 km^2. The carbonates have a gentle, <5°, dip to the NE and are affected by few regional, low displacement faults or folds. Despite their simple tectonic history, carbonates display ubiquitous open fractures, sub-vertical veins, and sub-vertical as well as sub-horizontal stylolites. Combining structural analysis, drone imaging, isotope studies and mathematical modelling, we reconstruct the fracturing history of the Jandaíra Formation during and following subsidence and analyse the impact fractures had on coeval fluid flow. We find that Jandaíra carbonates, fully cemented after early diagenesis, experienced negligible deformation during the first few hundreds of meters of subsidence but were pervasively fractured when they reached depths >400–500 m. Deformation was accommodated by a dense network of sub-vertical mode I and hybrid fractures associated with sub-vertical stylolites developed in a stress field characterised by a sub-horizontal σ_1 and sub-vertical σ_2. The development of a network of hybrid fractures, rarely reported in the literature, activated the circulation of waters charged in the mountainous region, flowing along the porous Açu sandstone underlying the Jandaíra carbonates and rising to the surface through the fractured carbonates. With persisting subsidence, carbonates reached depths of 800–900 m entering a depth interval characterised by a sub-vertical σ_1. At this stage, sub-horizontal stylolites developed liberating calcite which sealed the sub-vertical open fractures transforming them in veins and preventing further flow. During Tertiary exhumation, several of the pre-existing veins and stylolites opened and became longer, and new fractures were created typically with the same directions of the older features. The simplicity of our model suggests that most rocks in passive margin settings might have followed a similar evolution and thus display similar structures.

INTRODUCTION

The uppermost kilometres of the Earth are typically affected by compressional stresses essentially resulting from gravity and tectonic processes. This is the case not only in orogenic domains, but also in plate interiors and at passive continental margins (e.g. Heidbach *et al.*, 2010). Even in simplistic scenarios where overburden increases linearly with depth and where a depth-independent tectonic stress exists (e.g. Bell & Babcock, 1986), rocks subsiding from the Earth surface to depths of several kilometres experience different states of stress. These include changes in the spatial position of the principal stresses, of their magnitude and of the differential stress (itself exerting a major control on the occurrence of fracturing) (Zoback, 2007). Depending on the depth at which it experiences deformation, a subsiding rock might thus display very different types and spatial organisation of fractures.

Correspondence: Giovanni Bertotti, Department of Geoscience and Engineering, Delft University of Technology, Stevinweg 1, 2628CN Delft, the Netherlands. E-mail: g.bertotti@tudelft.nl

[1]Present address: King Fahd University of Petroleum and Minerals, College of Petroleum Engineering and Geosciences, Dhahran 31261, Saudi Arabia.

Borehole images and cores in flat-lying reservoirs document the occurrence of fracturing during subsidence (e.g. Lorenz *et al.*, 1991). For outcropping rocks, the traditional knowledge that most fractures are related to exhumation and, therefore, have little relevance for buried reservoirs, is being replaced by an increasing awareness that substantial fracturing takes place during subsidence (e.g. Lamarche *et al.*, 2012).

Understanding fracture patterns developed during basin subsidence provides constraints on the coeval stress field and facilitates prediction of permeability in naturally fractured reservoirs. Fracture networks can form efficient pathways for fluid circulation (e.g. Sibson, 2000) thereby playing a role, for instance, in hydrocarbons migration and storage. The architecture and topology of these networks are of key importance in controlling their impact on reservoir-scale flow properties (e.g. Sanderson & Nixon, 2015). In addition, fractures developed during subsidence provide distributed mechanical discontinuities which might be reactivated once rocks are subjected to a new stress field, for example related to depth changes and/or to folding.

Predicting fracture patterns in subsiding rocks, however, is not trivial as the knowledge of how stresses change with depth is affected by large uncertainties and because the degree and modality of fracturing are, among others, related to the mechanical properties of the rock which are expected to change with depth and time (e.g. Eberli *et al.*, 2003).

In this contribution, we present a model for the development of fracture networks in carbonate rocks during regional post-rift subsidence based on the analysis of well-suited outcrops. We show that syn-subsidence fracturing is important and led to the development of an extensive fracture network, opening pathways for regional flow which was eventually shut down by the cementation of the open fractures.

We focus on carbonate rocks because they typically experience early diagenesis and, therefore, are prone to fracturing already at shallow depths and because of the widespread occurrence of fracture-enhanced dissolution and cementation. We use outcrop data as they allow for a full characterisation of fracture types and spatial organisation, and of the associated fluid flow. Differently from most outcrop studies, we (i) investigate large outcrops ($>10^3$ m^2) spread over an area in excess of 10^2 km^2, (ii) strictly separate veins and stylolites from open fractures, and (iii) integrate structural results with isotope studies from the veins cements.

After having presented and interpreted the structural data, we reconstruct the stress field at the time when the structures formed and propose a general model for their development. Using isotopic data from veins, we then infer the main traits of the hydrogeological system that was activated as a consequence of fracturing. We finally compare our conclusions with other regions suggesting that our model can be applied to a variety of tectonically similar contexts. This implies that similar types and networks of completely sub-seismic fractures could be expected in comparable buried rocks in, for instance reservoirs for water and hydrocarbons.

FRACTURE PATTERNS IN THE JANDAÍRA FORMATION

Geological background

The data presented in this contribution originate from large outcrops of the Cenomanian-Turonian Jandaíra Formation,

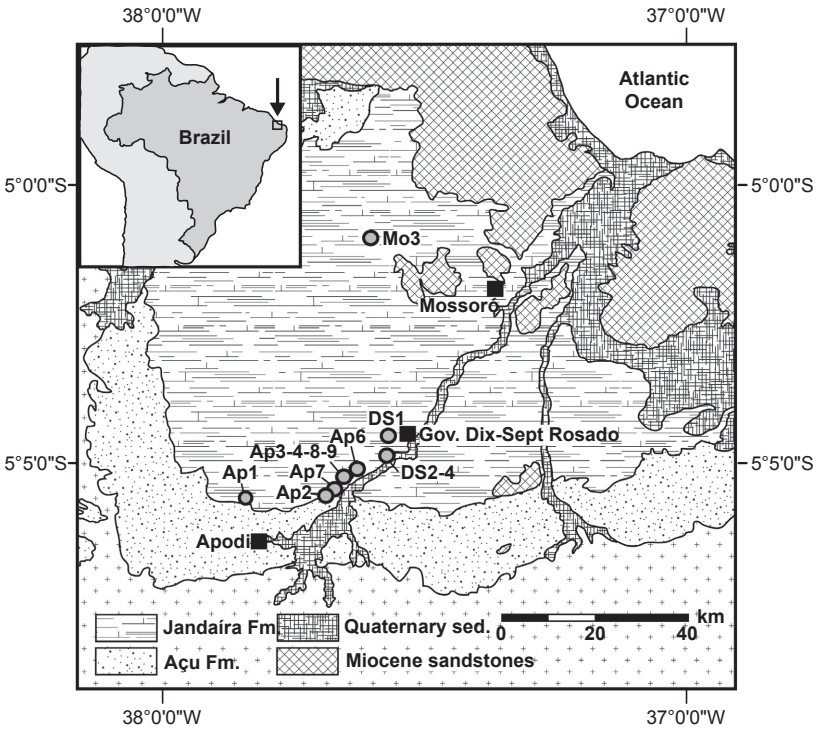

Fig. 1. Simplified geological map of the Potiguar basin with location the of the outcrops mentioned in the paper. The position of the study area is shown in the inset.

a shallow water carbonate succession (Tibana & Terra, 1981) deposited after the end of normal faulting in the Potiguar basin, NE Brazil, a failed arm of the Equatorial Atlantic ocean (de Matos, 1992; de Castro *et al.*, 2012) (Fig. 1).

Rifting in the Potiguar basins lasted from Neocomian to Barreniam times and led to the formation of a system of SW-NE trending half-grabens filled with an up to 4 km thick succession of mainly continental clastics (Pendencia Formation) (e.g. Costa de Melo *et al.*, 2016; Bertani *et al.*, 1990). Following the end of rifting at ca. 110 Ma and short-lived inversion in the Aptian, fluvial to transitional clastics (Açu Formation) and shallow water carbonates (Jandaíra Fromation) were deposited in Cenomanian and Upper Cenomanian to Turonian time respectively (Tibana & Terra, 1981; de Araripe & Feijó, 1994). Controlled by the thermal subsidence of the Potiguar and Equatorial Atlantic basins, thicknesses of the Açu and Jandaíra Formations increase and facies become more distal from SW where the basin was flanked by exposed basement, to the NE where kilometres of essentially marine sediments accumulated.

Vertical movements changed in the Tertiary when the onshore part of the basin began moving upward resulting in generalised gentle NE-ward dip. Roughly at the same time, a new stress field was established characterised by NW-SE trending compressional stress (Reis *et al.*, 2013).

The data set

We have investigated an approximately 30 × 20 km large region N of the city of Apodi (Rio Grande do Norte) (Fig. 1). Here, the Jandaíra Formation is composed of a 70–100 m thick succession of shallow water carbonates organised in few-decimeters-thick beds of predominantly grainstones overlying fluvial to transitional sandstones of the Açu Formation (e.g. Maraschin *et al.*, 2004). Rocks of the Jandaíra Formation are gently dipping to the N and devoid of major visible faults and/or folds thereby providing an excellent case study for phenomena taking place during regional subsidence. Evident fracture networks with variable patterns characterise all outcrops and are visible in satellite images.

Exposures in the region are generally of high quality, one of the few problems being the variable degree of karstification. In the area of interest, we have studied 13 pavements, typically hundreds of meters across with negligible vertical incision. Analysing km^2-size outcrops spread over an area of several hundreds of km^2 (Fig. 1), we capture fracture patterns associated with regional rather than local stresses caused, for instance by faults or folds.

In each outcrop, we have acquired fracture data from stitched and ortho-rectified images obtained with a 14 megapixel compact camera carried by an Unmanned Aerial Vehicle (UAV). Applying a flight altitude of 50 meters and an overlap between flights of ca. 70% we have achieved a resolution at the cm-scale. We improve the processing accuracy and speed by storing the drone and camera position for each image and integrating ground control points positioned with GPS and a Laser Range Finder. Images, image locations and control points are processed into high-resolution ortho-rectified outcrop maps using AgiSoft PhotoScan (Javernick *et al.*, 2014; Tavani *et al.*, 2014). Interpretation of the outcrop images is done by digitising all distinguishable features in a GIS environment using DigiFract software which has also been used to produce stereoplots and other relevant diagrams (Hardebol & Bertotti, 2013). We mapped >9,300 open fractures ranging in length from 0.5 m to hundreds of meters.

In 33 stations distributed in the various outcrops, we have acquired detailed structural data resulting in nearly 300 observations inclusive of veins and stylolites perpendicular and parallel to bedding (Table 1). We dedicated particular attention to the kinematics of veins, looking at the displacement of matching boundaries and, in thin section, at the internal structure of vein cements. To sample key sites like intersections between stylolites and veins we have used a drilling machine. As the main goal of this manuscript is to document the fracturing history of carbonates during subsidence, we did not measure systematically vein thicknesses. Apertures of barren fractures have not been recorded as they are influenced by exhumation and dissolution.

Structural elements

All investigated outcrops show widespread deformation structures. Features accommodating substantial strain are rare and generally limited to few normal and strike-slip faults with displacements of few meters. The dominant features are low-strain fractures pervasively distributed over the entire area. Beside open, generally barren, fractures, we observed stylolites (bedding-parallel and perpendicular) and veins (Fig. 2).

Sub-horizontal (=bedding-parallel) stylolites are several decimeters to a few meters long, with very well developed peaks (Fig. 2a) and are mainly visible in mudstones.

Table 1. Outcrops and structural stations in the Jandaíra formation used for this study

Outcrop	Coordinates	Stylolites samples
AP1	629916 9381503	
AP2	648176 9385026	
AP3	650636 9387810	
AP4	652108 9388522	HAM24 & 26
AP5	644376 9384942	
AP6	653815 9390089	
AP7	649034 9384915	
AP8	652064 9388699	
AP9	653392 9388629	
DS1	660311 9396042	
DS2	659906 9392295	
DS3	660747 9392368	
DS4	660645 9392124	
MO3	653815 9390089	HS 2

Sub-vertical (= bedding-perpendicular) stylolites are common and distributed over the entire area. They are up to a few meters long but only less than a few decimeters tall. They abut against bedding surfaces and, although observations are rare, seem to be overprinted by bedding-parallel stylolites. Sub-vertical stylolites, compared with the sub-horizontal counterparts, have less well pronounced peaks. Sub-vertical stylolites display a well-clustered orientation generally trending E-W to WNW-ESE (Fig. 3), which documents a N-S to NNE-SSW-trending sub-horizontal compression. In a few stations (e.g. outcrops AP2 and AP7) mainly localised in the SW reaches of the area, we observed a second subordinate set of sub-vertical stylolites oriented NE-SW. This second set developed during Tertiary shortening (e.g. Reis *et al.*, 2013) and is not further discussed here as it is unrelated to regional subsidence.

Veins are all sub-vertical (perpendicular to bedding), several meters long, up to a few decimeters tall, and can be up to few centimeters thick. Thin (<2 mm) veins (Fig. 2b) typically display matching opposing walls documenting the lack of dissolution prior to cementation. Thicker veins, on the contrary, have more irregular, not-–matching walls (Fig. 2c). Veins often stop at bedding surfaces and, in most visible cases, against bedding-parallel stylolites. Veins consistently strike N-S to NNE-SSW across the entire study area (Fig. 3). Similarly to what is observed for the sub-vertical stylolites, a second subordinate directional set is present in a few outcrops, which is probably associated with Tertiary compression (Reis *et al.*, 2013) and will not be further discussed here. All veins have a similar infill composed of generally blocky calcite crystals with similar optical and cathodoluminescence properties.

Structural features such as restraining and releasing bends show that a significant number of veins opened with a shear component (Fig. 2d). Veins display both dextral and sinistral senses of shear and are organised in conjugate sets. We have measured dihedral angles of 16–21° (Fig. 3). Because of these low dihedral angles, plots of veins directions give the impression of an orientation scatter, hiding, however, the fact they are conjugate. Because of their mixed mode and of the low-interfault angle, veins are interpreted as hybrid fractures (e.g Hancock, 1985; Sibson, 2000; Belayneh & Cosgrove, 2010).

Spatial relations between the different structures can be constrained in a number of stations (Fig. 4). In stations AP9.1 and DS4.1, for instance, stylolites are observed with a N110 strike which we associate with a N20 striking maximum compressional stress. This direction is compatible with the hybrid veins for which a sense of movement could be determined as well as for the other veins which opened perpendicular to the fracture walls (mode I). In a few cases (see for instance outcrop AP9.1), veins have been observed which are kinematically linked to stylolites documenting how they were operating at the same time.

Implications for state of stress during fracturing

We associate the observed structures with two different states of stress, dictated by the presence of sub-vertical and sub-horizontal stylolites. Sub-vertical stylolites

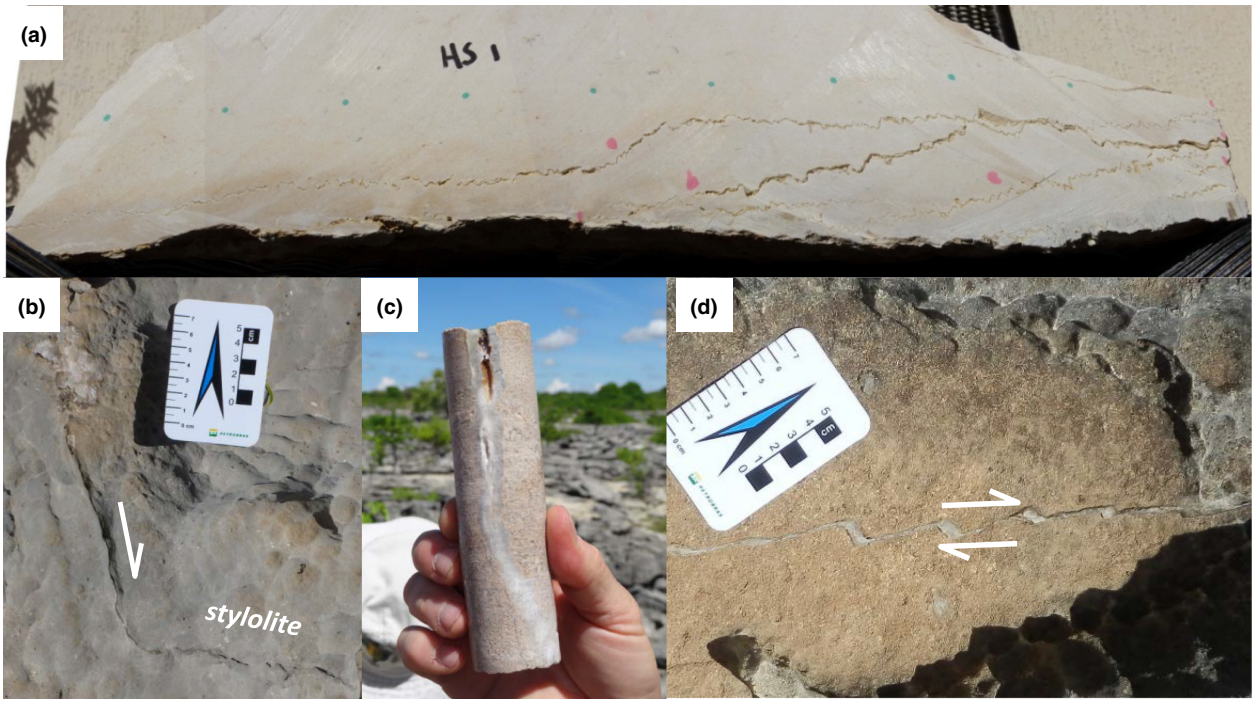

Fig. 2. Structures observed in the Jandaíra Formation. (a) sub-horizontal stylolites (sample H1, outcrop MO3); the sample has been used for depth calculation. (b) hybrid vein kinematically associated with a roughly E-W striking stylolitic surface exposed on a sub-horizontal pavement (outcrop AP4). (c) thick vein with non-matching boundaries (outcrop AP1). (d) hybrid vein with dextral sense of movement exposed on a horizontal pavement of outcrop AP4.

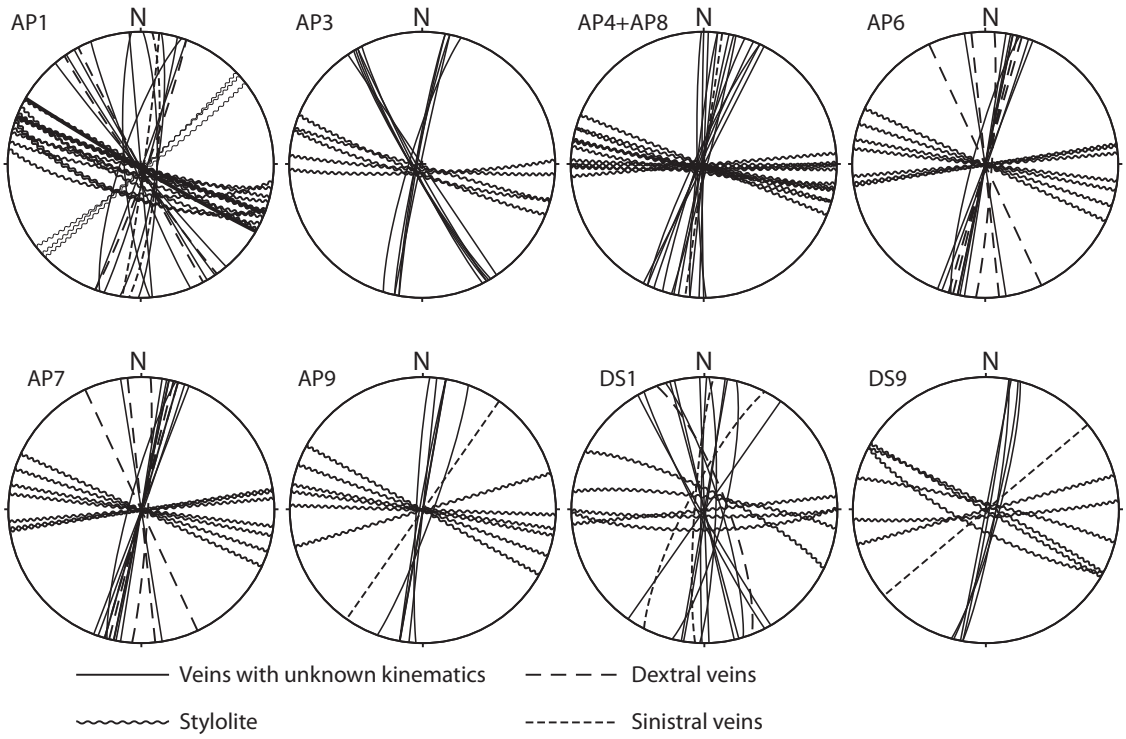

Fig. 3. Stereoplots showing the position of sub-vertical veins and stylolites in 8 representative outcrops of the study area. Outcrop location is shown in Fig. 1.

formed with a sub-horizontal, roughly N-S directed maximum principal stress σ_1. Conjugate sub-vertical veins are compatible with the same direction of maximum compressional stress and further document a sub-vertical position of σ_2 parallel to the intersection between the hybrid fractures (Figs 3 and 4). The kinematic link between veins and stylolites is graphically documented in outcrops such as the one in Fig. 2c where the hybrid vein merges in E-W trending stylolite.

The second stress field was associated with the development of sub-horizontal stylolites observed all over the area of study (Fig. 3) and, possibly, of some of the veins for which no sense of movement or diagnostic angular relations could be determined. This second stress field

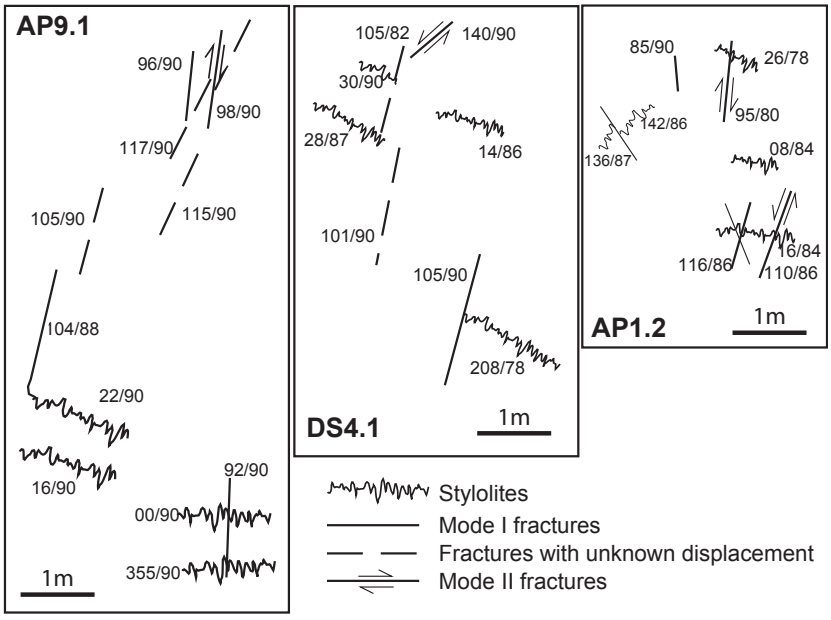

Fig. 4. Detailed structural maps of three different stations in outcrops AP1, AP9 and DS4 showing the relative position of (hybrid) veins and stylolites. Note how most of the observed structures can be associated with a stress field characterised by a NNE-SSW trending σ_1 and a sub-vertical σ_2. The frames are roughly 5 m across; in all maps, North is upward.

was characterised by a sub-vertical position of the maximum principal stress.

The type of fractures and the orientation and position of the stylolites and veins observed in the outcrops of the Jandaíra Formation are very consistent over distances of tens of kilometres (Figs 1 and 3) thereby suggesting that the causative stresses are of regional and not local nature.

STRESS AND STRAIN DURING SUBSIDENCE

Reference scenarios for principal stresses in depth

Having documented the structures developed in the Jandaíra carbonates, we use simple models to assess the stress field in which they formed. Two different simplistic scenarios can be envisaged for the stress field acting on upper crustal rocks in a passive continental margin, one where the only force is gravity and one where a far-field sub-horizontal stress is also present. This sub-horizontal component could be of tectonic origin or related to lateral pressure changes caused by lateral thickness and density variations predicted in some passive continental margins (Pascal & Cloetingh, 2009).

Principal stresses in a gravity-only scenario

The gravity-only scenario is based on the assumption that gravity is the only source of stress. In this case, i) the maximum principal stress σ_1 is always vertical and controlled by the overburden, and (ii) stresses on the horizontal plane are axial symmetric with their magnitude being controlled by the Poisson effect exerted by the vertical stress (Fig. 5a). If rock density and Poisson's ratio remain constant, all stresses increase linearly with depth with the horizontal stresses being roughly 1/3 of the vertical one resulting in (i) a normal fault stress regime at all depths and, (ii) a deviatoric stress starting at 0 at the surface and constantly increasing with depth.

Principal stresses in a gravity-tectonic scenario

The second scenario includes a sub-horizontal far-field stress, which we conventionally call tectonic stress. To predict the distribution of stress at depth we make the following simplifying assumptions: (i) the surface of the Earth is a free surface, (ii) the stress in the vertical direction (z in the model) corresponds to the overburden and increases linearly with depth, (iii) the stress acting in the y direction, parallel to the far-field stress, results from the tectonic stress increased by the Poisson's effect of overburden, and (iv) the stress in the x direction corresponds to the Poisson's effects caused by gravity and by the tectonic stress. The corresponding state of stress tensor is provided in Eqn (1):

$$\begin{matrix} \frac{\nu}{1-\nu}\rho g z + \frac{\nu}{1-\nu}S_{\text{tect}} & 0 & 0 \\ 0 & \frac{\nu}{1-\nu}\rho g z + S_{\text{tect}} & 0 \\ 0 & 0 & \rho g z \end{matrix} . \quad (1)$$

Results for representative parameters (specified in Table 2) are shown in Fig. 5b. Because of their different values at 0 m depth and of their different slopes, the stress curves associated with the three directions will cross each other thereby predicting changes in the position in space of the principal stress with depth although the applied boundary stresses remain constant. In the structural geology jargon, these changes are called permutations.

On the basis of the model of Fig. 5b, we identify three depth intervals characterised by different positions in space of the principal stresses. In the uppermost interval, σ_1 coincides with the far-field stress, σ_2 is sub-horizontal and perpendicular to it and σ_3 is vertical coinciding with gravity. At deeper levels, below the intersection between the S_v and S_x curves, the maximum principal stress remains parallel to the far-field stress, but σ_2 acquires a vertical position, while σ_3 is now sub-horizontal and perpendicular to the far-field stress. At depths larger than the S_y and S_v crossing, the maximum compressional stress is vertical while σ_2 corresponds to far-field stress

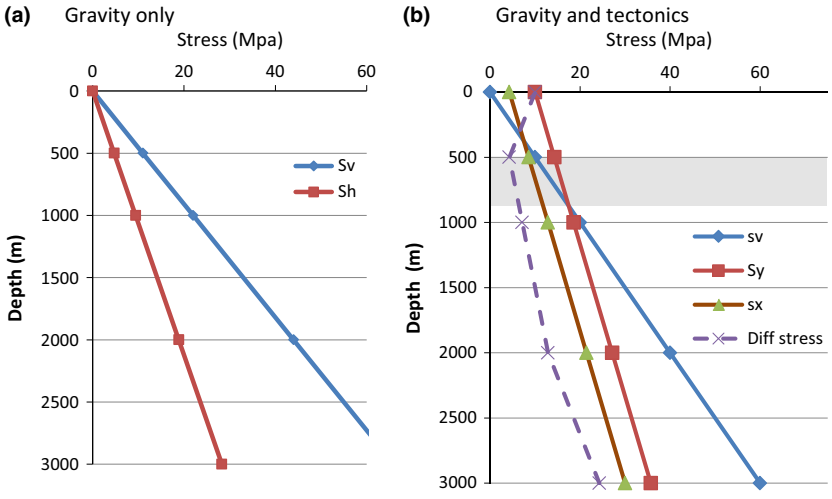

Fig. 5. Simplified distribution of vertical and horizontal stresses in a gravity-only (left) and gravity-and-tectonic scenarios (right). The grey bar in 5b corresponds to the depth interval where σ_2 is vertical. Parameters are provided in Table 2.

Table 2. Parameters used for stress vs. depth plots of Fig. 5

		Preferred model	Range of values used for sensitivity
Density (kg m^{-3})	ρ	2200	2000–2600
Poisson's ratio	ν	0.3	0.3
Tectonic stress (MPa)		10	0–35

and σ_3 is sub-horizontal and perpendicular to it. The driver behind these changes is overburden, which is 0 MPa at the surface and increases at a rate higher than that of other stresses and which, at a certain depth, will necessarily become the maximum compressional stress.

Despite its obvious simplified nature, our model shows that a rock subsiding from the surface to depths of several hundreds of meters will experience fundamentally different stress conditions despite the absence of regional changes. The depths of these changes obviously depend on the parameters adopted (see Fig. 5b for details); their existence, however, is a necessary consequence of the different slopes and of the ever-increasing gravity load with depth.

Depth of formation of Jandaíra veins and stylolites

Depth of formation of sub-vertical veins

We have shown that sub-vertical stylolites and associated (conjugate) veins (Fig. 3) formed as a result of a stress field characterised by a sub-horizontal σ_1 and a sub-vertical σ_2. Such a setting is incompatible with a gravity only scenario (Fig. 5a) and is only realised in the intermediate depth level of the gravity-tectonic scenario (grey bar in Fig. 5b). In the reference model the interval lies at depths between ca. 500 and 800 m (see Fig. 5b and Table 2 for the adopted parameters).

The depths of the upper and lower boundaries of the interval where σ_2 is vertical, are a function of the magnitude of the tectonic stress and of density (Fig. 6). The largest impact is exerted by the intensity of the horizontal (tectonic) stress: the stronger this is, the deeper the interval will lie. Increasing densities, on the contrary, result in minor shallowing of the relevant depth interval.

Depth of formation of sub-horizontal stylolites

Sub-horizontal stylolites are associated with a sub-vertical maximum compressional stress. As the vertical stress is related to gravity, its magnitude can be used to infer the depth at which stylolites formed. A currently used method to determine the intensity of the stress causing stylolite formation is based on the notion that the wavelength content of a stylolite results from the competition between the elastic energy of the rock (favoring short wave-lengths) and the surface tension (enhancing long wave-lengths) (Schmittbuhl *et al.*, 2004). In a Fourier Power Spectrum, the wavelengths of the two domains intersect at a value called cross-over length L_c (Ebner *et al.*, 2009). The cross-over length is linked to the causative stress by the equation:

$$L_c = \frac{\gamma E}{\beta \sigma_{\text{mean}} \sigma_{\text{differential}}}. \quad (2)$$

where γ is the surface tension, E the Young modulus, σ_m and $\sigma_{\text{differential}}$ the mean and differential stress respectively, and β defined below (see also Table 2).

$$\beta = \frac{2v(1-2v)}{\pi}.$$

This relation, however, is only valid when gravity is the only stress present. To include settings with a horizontal stress we have modified Eqn (2) including a tectonic stress σ_{tect} which results in new values of the mean and differential stresses.

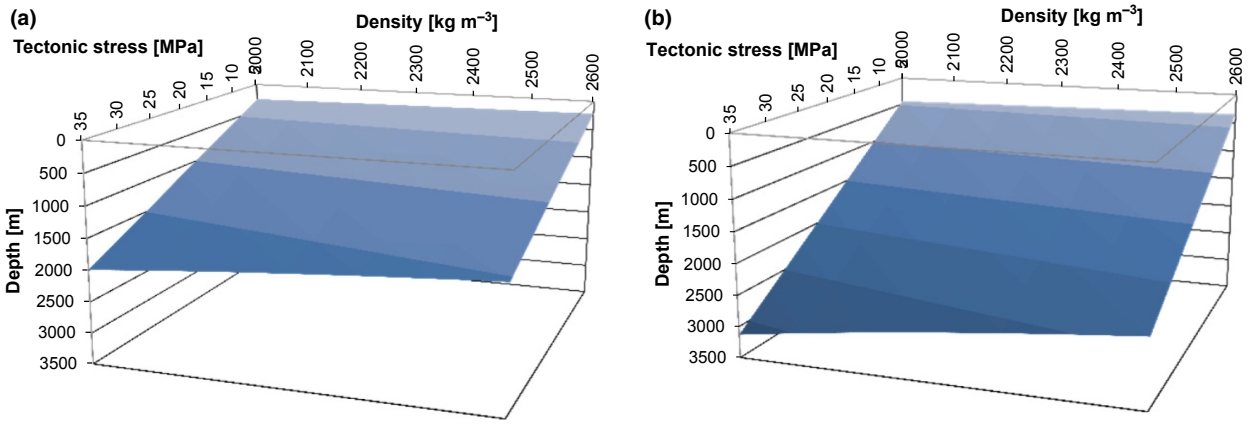

Fig. 6. Position of the upper and lower surfaces of the depth interval characterised by a vertical σ_2 as a function of tectonic stress and density (panels a and b, respectively).

$$\sigma_m = \frac{1}{3}\left(\sigma_{zz} + 2\frac{\nu}{1-\nu}\sigma_{zz} + \frac{\nu}{1-\nu}\sigma_{tect} + \sigma_{tect}\right)$$

$$\sigma_{differential} = \sigma_{zz} - \left(\frac{\nu}{1-\nu}\sigma_{zz} + \frac{\nu}{1-\nu}\sigma_{tect}\right).$$

Introducing σ_m and $\sigma_{differential}$ into Eqn (2), one obtains a new equation relating the cross-over length to the boundary stresses and the mechanical parameters:

$$L_c = \frac{\gamma E}{\beta\frac{1}{3}(a\sigma_{zz}^2 + b\sigma_{zz} - c)} \quad (3)$$

where

$$a = 1 + \left(\frac{v}{1-v}\right) - 2\left(\frac{v}{1-v}\right)^2$$

$$b = \sigma_{tect} - 3\sigma_{tect}\left(\frac{v}{1-v}\right)^2 - \sigma_{tect}\left(\frac{v}{1-v}\right)$$

$$c = \left(\frac{v}{1-v}\right)^2 {\sigma_{tect}}^2 + \left(\frac{v}{1-v}\right){\sigma_{tect}}^2.$$

Solving Eqn (3) for specific parameters and Lc measurements, the vertical stress (σ_{zz}) during stylolite formation is obtained which can be then translated in depth assuming a density distribution.

Samples were cut and polished, the trace of the stylolites was digitised on an image taken from the slab and Fourier Power Spectra were created for all stylolites. To extract values of the vertical stresses and the corresponding depths of stylolite formation we have adopted parameters shown in Table 3.

We have successfully analysed four sub-horizontal stylolites from three different samples, two from the area around Apodi and one from the Mossoro region (see Table 1). The values obtained for the different samples are well comparable confirming the reliability of the method and of our measurements. An example of the results from representative sample HS2a is shown in Fig. 7.

Table 3. Parameters used for stress calculations. Sources are as follows. Surface tension: Ebner *et al.*, 2009; Young's modulus : Reis *et al.* (2013) and http://www.jsg.utexas.edu/tyzhu/files/Some-Useful-Numbers.pdf

		Preferred model	Range for sensitivity analysis
Surface tension (J m^{-2})	Υ	0.27	0.27
Young's modulus (GPa)	E	25	15–55
Poisson's ratio	ν	0.3	0.3
Rock density (kg m^{-3})	ρ	2200	2000–2600
Tectonic stress (MPa)		10	10–30
Crossover-lengths (m)	L_c	Derived from FPS analysis	

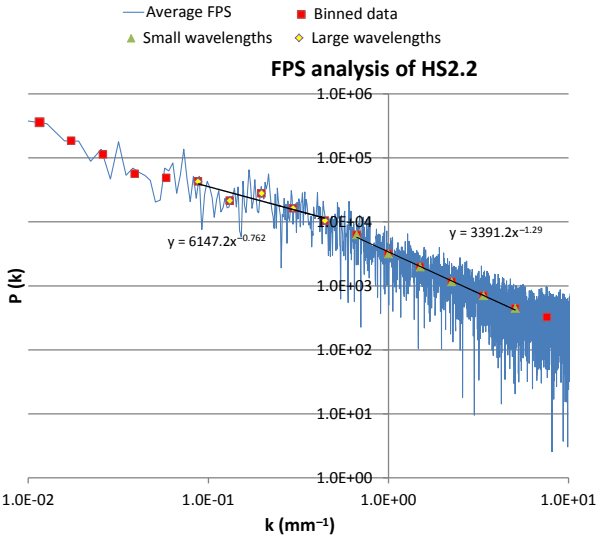

Fig. 7. Fourier Power Spectrum (FPS) analysis for stylolite HS2a. Symbols are as follows. Blue line, original FPS data; red squares, averaged data; yellow diamond and green triangles are points used to fit the trend lines for respectively the small and large wavenumbers. The equations for the trend lines are given in the graph. The crossover-length lies at 1/k = 6.4 mm.

Results from all measurements are displayed in Table 4. Assuming a tectonics stress of 10 MPa comparable to the one adopted to estimate the depth of formation of sub-vertical conjugate veins, we obtain depths between 632 and 827 m (average values of minimum and maximum values for all sample) (adopted parameters are shown in Table 3). These values increase by assuming stronger tectonic stresses (Table 4).

Relative age of sub-vertical and sub-horizontal structures

From the previous analysis, we have obtained depths for the formation of sub-vertical conjugate hybrid veins and for the development of sub-horizontal stylolites. A plot of the two data sets (Fig. 8a) shows that most of the admissible depths for the conjugate structures are shallower than those obtained for the generation of stylolites. The overlap between the two domains should result from various uncertainties as sub-vertical conjugate fractures and sub-horizontal stylolites require different positions of the maximum principal stress and, therefore, cannot be formed at the same time.

In most samples, sub-horizontal stylolites overprint and are therefore younger than the veins (e.g. Fig. 8b). In terms of principal stresses, this suggests that the rocks experienced first a stress configuration characterised by sub-horizontal σ_1 and sub-vertical σ_2 leading to the formation of sub-vertical mode I and mode I – mode II conjugate veins (and stylolites), and then, at larger depths, by one in which the maximum principal stress had become vertical causing the formation of sub-horizontal stylolites. This succession of deformation is perfectly compatible with what has been predicted for a rock subsiding through

Table 4. Vertical stresses and formation depths resulting from stylolite analysis (parameters are shown in Table 3). Sample location is indicated in Table 1 and Fig. 1

	HAM24.1			HAM26.1			HAM26.2			HS2a		
Tectonic stress	Min	Average	Max	Min	Average	Max	Min	Average	Max	Min	Average	Max
Vertical stress												
T = 0	7.4	10.5	16.6	10.9	14.0	21.2	6.6	9.8	14.8	6.7	9.5	14.3
T = 10	11.9	14.5	20.4	14.8	17.9	25.3	11.2	13.9	18.7	11.3	13.6	18.2
T = 20	18.8	20.6	25.1	20.8	23.1	29.2	18.4	20.1	23.7	18.5	20.0	23.3
T = 30	26.7	27.9	31.4	28.1	29.8	34.7	26.4	27.6	30.3	26.4	27.5	30.0
Stlylolite formation depth (m)												
T = 0	292	487	845	426	650	1082	259	454	756	264	442	731
T = 10	465	672	1041	581	827	1288	440	642	951	444	632	926
T = 20	738	954	1280	816	1069	1487	723	933	1207	725	926	1188
T = 30	1046	1295	1601	1102	1381	1771	1035	1279	1544	1037	1274	1529

a gravity-and-tectonics stress field as modelled in Fig. 5b suggesting that the switch from one mode of deformation to the other was simply controlled by increasing subsidence.

FRACTURING AND FLUID CIRCULATION

Wholesale deformation of the Jandaíra carbonate platform during subsidence was accommodated by the generation of a very large number of sub-vertical mode I and hybrid fractures, and stylolites distributed over an area of hundreds of km^2 (see distribution of outcrops in Fig. 1). As a consequence, the carbonates of the Jandaíra Formation became highly permeable allowing for the onset of transient circulation which ended when the open fractures were cemented. In this chapter, we estimate fracture-related permeability changes and infer characteristics of the circulating waters (e.g. de Graaf *et al.*, 2017).

Porosity and permeability changes

As a result of early cementation, the carbonates of the Jandaíra Formation had lost most of their primary porosity when they started their subsidence (de Graaf *et al.*, 2017). This is supported by the observation that veins systematically cut grains and sparitic cements in the rock.

To provide a rough estimate of the change in porosity and permeability caused by activation of the fracture network, we have analysed a relatively small pavement (few tens of meters across; part of outcrop AP6) which displays few barren fractures and a large number of veins and stylolites which escaped reactivation and opening during exhumation (Fig. 9).

Using spacing, orientation and length distributions we derive an average fracture porosity, defined as the ratio between aperture, multiplied by fracture length, and outcrop area. As measuring the thickness of all veins along their entire length would have been a daunting task not justified in this study, we have estimated apertures during fracturing using a sub-linear length-aperture scaling method (Olson, 2003; Bisdom *et al.*, 2016). The modelled aperture is between 0 and 2 mm for most fractures, and up to 5 mm for some of the largest fractures (Bisdom *et al.*, 2016). This modelled range corresponds to qualitative observations of vein widths made in the outcrop. We obtain that the fracture-related porosity is in the order of 0.1–0.2%. Other pavements provided similar values.

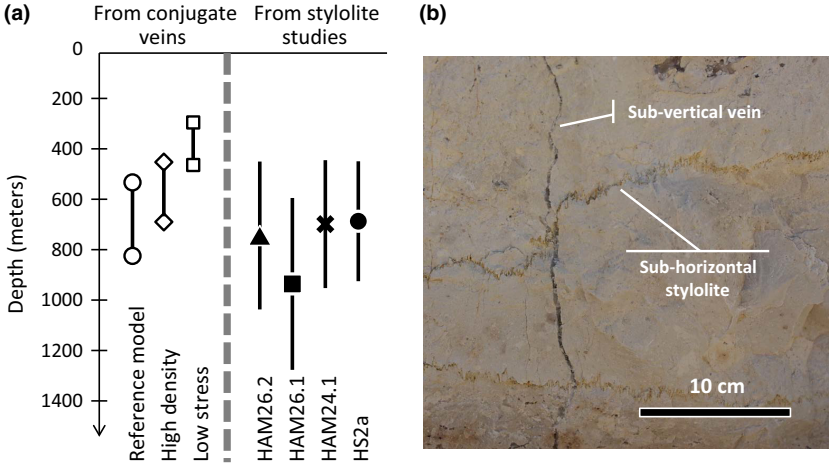

Fig. 8. Depth of formation of sub-vertical hybrid veins and sub-horizontal stylolites (a) and image of sub-horizontal stylolite overprinting a sub-vertical vein (b). Depths of formation of hybrid veins are derived from the diagram of Fig. 5b and the related sensitivity analysis (Fig. 6); methods used to determine the depth of formation of sub-horizontal stylolites are explained in text.

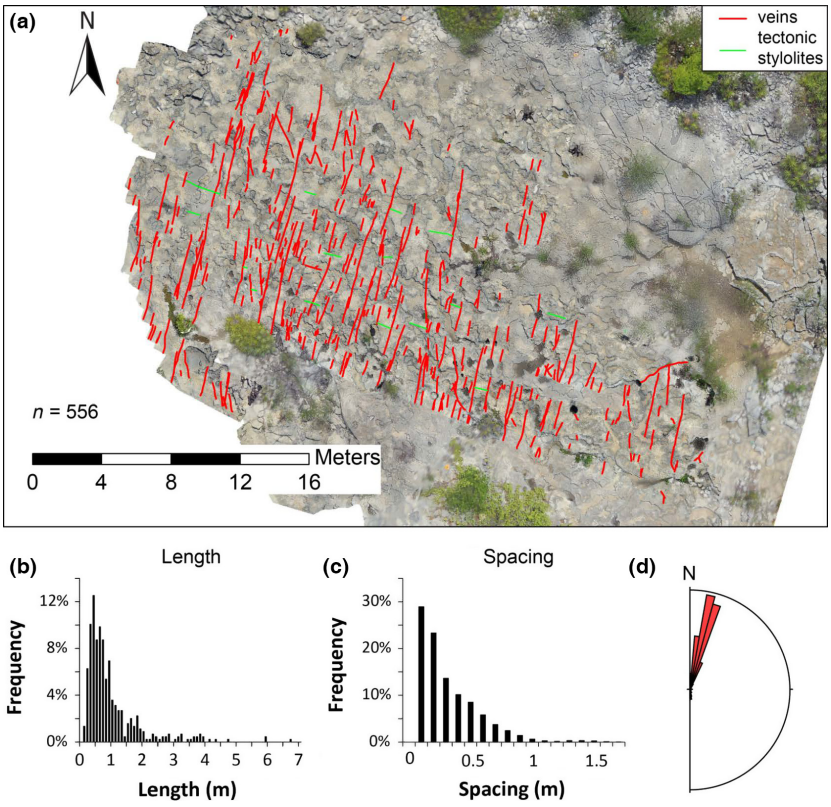

Fig. 9. The pavement (outcrop AP6) used to define geometric characteristics of sub-vertical veins and stylolites not reactivated during exhumation. (a) the pavement imaged from the drone: veins and stylolites are indicated with red and green lines respectively. (b) length distribution of veins; (c) vein spacing; (d) rose diagram of vein strike.

Effective permeability is quantified using the cubic law in the directions parallel and perpendicular to the maximum horizontal stress (S_{Hmax}) (Snow, 1969). Assuming a representative low permeability rock matrix of 1 mD, and using the modelled aperture distribution, the effective permeability parallel to S_{Hmax} is up to ten times larger than matrix permeability, whereas in the direction of S_{hmin}, there is no flow. In the vertical direction many fractures are seen to continue through several thick beds of the Jandaíra Fm., indicating that fractures cut through thick mechanical units, thereby providing high vertical connectivity. In this dimension, the high-intensity fracture networks can create effective permeabilities of up to 1 Darcy.

The circulating fluids

Strictly speaking, the only record we have of the fluids which circulated in the fracture network developed at hundreds of meters depth during subsidence, is provided by the cement (mineralisation) precipitated in the previously open fractures. This transformed the open fractures in veins and, thereby, caused the end of flow. In the following section, we use isotopes from the country rock and the veins to extract information on the nature of the (last) fluids circulating through the network.

Methodology

After standard petrographic analysis, the calcite cement of the veins was analysed for stable carbon and oxygen isotopes (Duhr & Hilkert, 2004). Calcite material was sampled with a Merchantek Micromill from 200 μm thin sections and measured using an automated sampling device (GASBENCH II). Around 10 μg of carbonate material was digested in concentrated anhydrous phosphoric acid. The released CO_2 gas was subsequently transported by a He carrier flow to a continuous flow isotope ratio mass spectrometer (Thermo Finnigan Delta+) for analysis of $\delta^{13}C_{VPDB}$ and $\delta^{18}O_{VPDB}$.

Fluid inclusions isotope analysis was performed to obtain values for $\delta^{2}H_{VSMOW}$ and $\delta^{18}O_{VSMOW}$ of the water from which the veins crystallised. Vein samples of 0.4 to 2 g were isolated from the cores and crushed at 110°C in the Amsterdam Device (Vonhof *et al.*, 2006). Waters released from the inclusions in the cement during crushing were subsequently decomposed in H_2 and CO in a TC-EA reactor tube. These two gases are chromatographically separated before entering in a continuous-flow isotope-ratio mass spectrometer (ThermoFinnigan Delta XP) capable of measuring both $\delta^{2}H_{VSMOW}$ and $\delta^{18}O_{VSMOW}$ values from one water release due to a rapid magnet peak jump between the entries of both the H_2 gas and the CO gas.

Results of stable isotope analysis

We performed successful measurements on the micrite, the sparite filling the rock pores and on the veins. The results of the analyses show that the isotopic compositions of the micrite and pore-filling sparite of the host rock, and

the veins fall in three different though partly overlapping fields (Fig. 10a).

The micrite of the host rock covers a wide range of values with a clear positive relation between $\delta^{18}O_{VPDB}$ and $\delta^{13}C_{VPDB}$. The highest values (0‰ $\delta^{18}O_{VPDB}$ and 2‰ $\delta^{13}C_{VPDB}$) represent carbonate deposition in a marine environment; the trend towards lower values (−11.47‰ $\delta^{18}O_{VPDB}$ and −2.70‰ $\delta^{13}C_{VPDB}$) is interpreted as the result of early diagenesis in a fresh groundwater system (Hoefs, 1973; Hudson, 1977).

The sparite deposited in primary porosity of the Jandaíra carbonates has well clustered $\delta^{18}O_{VPDB}$ values, coinciding with the lowest $\delta^{18}O_{VPDB}$ values of the micrites, suggesting that the sparites precipitated from the same meteoric waters that caused early diagenesis of the micrites. The range in $\delta^{13}C_{VPDB}$ values is similar to that of the micrite confirming the interpretation that the pore-filling sparite precipitated during early diagenesis as a result of host rock dissolution.

Results from the 20 veins we have analysed (Table 1; Fig. 10a) (de Graaf *et al.*, 2017) document well clustered $\delta^{18}O_{VPDB}$ values that vary from −10.66 to −7.19‰, overlapping with the lower range of $\delta^{18}O_{VPDB}$ values observed in the host rock micrites. These values are consistent across the entire region and we have found no significant differences between cements in thin veins with matching walls and in thicker veins where important dissolution occurred prior to cementation.

$\delta^{13}C_{VPDB}$ values, on the contrary, are scattered and can be significantly lower than what is measured from the host rock. The range of $\delta^{13}C_{VPDB}$ values is not regionally correlated and is found also in transects across single veins. We interpret the $\delta^{13}C_{VPDB}$ signature of the veins as associated with the addition of bio-degradational carbon species that possibly originated in the underlying continental Açu Formation. Isotope values of sampled veins are clearly distinct from those of the sparite samples compatible with the observation that veins systematically cut the host rock, and strengthening the interpretation that precipitation in the primary porosity and in the veins was associated with two substantially different hydrogeological systems.

Further information on the origin of the fluids has been obtained from the isotope composition of fluid inclusions. Successful measurements were performed on 10 veins. Values for $\delta^{18}O_{VSMOW}$ vary from −5.3 to −3.5‰, and the $\delta^{2}H_{VSMOW}$ of the included water displays a range of −36.4 to −16.2‰. Once plotted on Global Mean Water Line (GMWL) (Craig, 1961), which describes the isotopic evolution of meteoric water as clouds progressively rain out, values from the veins of the Jandaíra Formation fall very close to the GMW line suggesting that the precipitating fluid had a meteoric origin (Fig. 10b) (Hoefs, 1973).

Fluid characteristics

The very homogeneous oxygen isotopic composition of all veins measured in the 30 × 20 km wide area NE of Apodi (Fig. 10) shows that the precipitation of calcite in the veins was associated with one single type of fluid that circulated through the fracture system. Indeed, cements measured in veins from the area of Mossoro, ca. 50 km N of the study area also have a similar composition (de Graaf *et al.*, 2017). The homogeneous isotopic signature of fluids precipitating calcite in veins spread of such a large area requires a basin-scale flow controlled by regional topography and temperatures rather than associated, for instance, with much more localised features such fault zones.

The fluid inclusion data show that the incorporated fluids were of meteoric nature and not marine waters trapped in the rock during sedimentation and expelled when fractures were formed. This is also compatible with

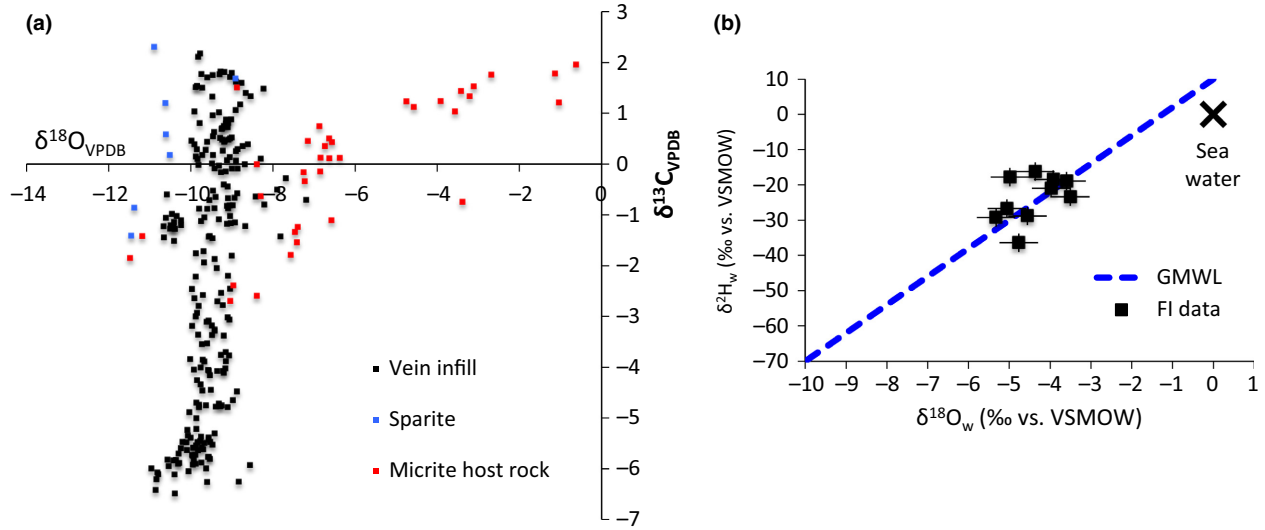

Fig. 10. (a) Oxygen and Carbon stable isotope data from calcite vein infill, and micrites and pore-filling sparites from the host rock. (b) Oxygen and Hydrogen isotopes of the veins fluid inclusions plotted against the Global Meteoric Water Line (GMWL).

the observation that the carbonates were fairly tight prior to fracturing, most of the primary porosity having been occluded by sparitic cement with a meteoric isotopic signature (Fig. 10a).

SUBSIDENCE, FRACTURING AND FLUID FLOW

We have shown that, during their regional subsidence, the Jandaíra carbonates experienced the formation of networks of sub-vertical veins and stylolites followed by their deactivation and overprinting by sub-horizontal stylolites. Using the scheme provided in Fig. 11 we present a reconstruction of the structural and hydrogeologic evolution of the rocks of the Potiguar basin during its post-rift evolution.

Prior to fracturing: from 0 to 500 m

Overlapping with deposition and early diagenesis, the limestones of the Jandaíra Formation subsided driven by post-rift thermal relaxation (Mello, 1989; Couto Anjos *et al.*, 1990). According to the stress model shown in Fig. 5b (see the caption and Table 2 for the adopted parameters), the upper 400–500 m crustal depths were characterised by a sub-horizontal position of the maximum principal stress σ_1. Following an Andersonian approach, sub-horizontal mode I fractures and/or low-angle reverse faults would be predicted, but none of this is observed. Apparently, no deformation affected the Jandaíra limestones in the first 400–500 m of their subsidence.

Having experienced early diagenesis and cementation, and only limited fracturing, the carbonates of the Jandaíra Formation functioned as an aquitard forming the upper boundary of the efficient aquifer associated with the Açu sandstone, which even at present has porosities of up to 30%. In our hydrogeological model, the aquifer was charged in the SW where the Açu sandstones were outcropping between the mountains and the carbonates of the Jandaíra Formation and, possibly, along boundary faults (e.g. Bertani *et al.*, 1990). The waters entering the subsurface, flowed along the Açu aquifer towards the NE, to the deep parts of the basin (Fig. 11a). The presence of meteoric waters in the Açu Formation in Cretaceous times is documented by the growth in phreatic conditions of authigenic feldspars around detrital orthoclase and microcline grains prior to the mechanic infiltration of smectite grains (Maraschin *et al.*, 2004).

Wholesale fracturing: between 500 and 800 m

The previously tight carbonates of the Jandaíra Formation experienced wholesale fracturing when they entered the depth interval characterised by a sub-vertical σ_2 (Fig. 11b). According to our modelling exercise, this occurred when the rocks were buried deeper than 500 m (Fig. 5b).

When deformation took place, an area in excess of 1000 km^2 was affected by distributed fracturing with the

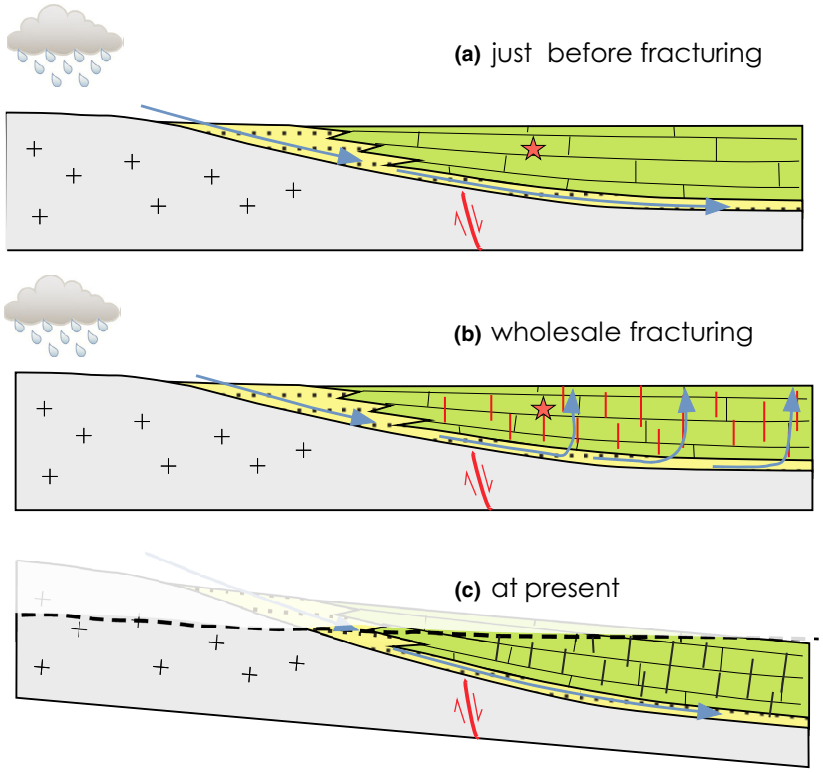

Fig. 11. The three main stages of the structural and geo-hydrological evolution of a transect along the axis of the Potiguar basin; the red star represents the general position of the studied rocks through time. (a) prior to fracturing, the Jandaíra formation acted as an aquitard; waters falling in the relief to the SW of the Potiguar basin entered the basin flowing along the porous Açu Sandstone; (b) with the activation of the regionally distributed fracture network, permeability in the Jandaíra carbonates increased and fluids flowed upward probably up the surface; once cement was precipitated in the veins, the Jandaíra rocks behaved again as aquitard. (c) Tertiary tilting caused the exhumation of the examined rocks to the surface and the present day geometry and structure.

development of a dense network of sub-vertical mode I and hybrid fractures and sub-vertical stylolites associated with a roughly N-S trending σ_1. The establishment of a network of fractures with significant opening component had a great impact on the hydrological system providing new pathways through the Jandaíra Formation. In our interpretation, the waters charged in the SW, flowing mostly along the Açu sandstones could then move upward through the Jandaíra carbonates probably reaching the surface (Fig. 11b).

How long this hydrological system remained active is difficult to determine. The occurrence of significant dissolution along the walls of thick veins prior to calcite precipitation (Fig. 2b) suggests that fractures remained open for a significant amount of time. This is compatible with the observation that the largest majority of veins display blocky calcite crystals suggesting that the veins were open when calcite started precipitating (Bons *et al.*, 2012).

Following fracturing: deeper than 800 m

With persisting subsidence, the presently outcropping rocks of the Jandaíra Formation left the depth interval characterised by a sub-vertical σ_2 and entered the domain where the maximum principal stress σ_1 acquires a vertical position (Fig. 5b). This induced the activation of a regional system of bedding-parallel stylolites overprinting the older sub-vertical veins and stylolites (Fig. 8b).

The occurence of massive of pressure solution along the sub-horizontal stylolites provided the calcite that precipitated in the open fractures and eventually transformed them in veins and thereby dramatically reducing the porosity and permeability of the Jandaíra Formation. Hydrological and petroleum-related studies show that in the entire region, the Jandaíra Formation acts presently as an aquitard (Morais-Neto *et al.*, 2009).

From maximum burial depth to present

Subsidence in the offshore portion of the Potiguar basin persisted until recent times and the Jandaíra formation is presently at depths >2000 m (de Araripe & Feijó, 1994). On the contrary, vertical movements in the area where the Jandaíra Formation is outcropping, switched from downward to upward at a poorly constrained moment, probably during the Miocene (e.g. Nogueira *et al.*, 2015) bringing to the Earth's surface the carbonates with veins and stylolites (Fig. 11c).

DISCUSSION

The activation and mode of fractures

We have shown that rocks of the Jandaíra formation subsided through the first 400–500 m of the crust without noticeable deformation and experienced significant fracturing only when the vertical stress had increased enough to become the intermediate principal stress. As the carbonates had only very limited porosity after early diagenesis, we conclude that pore pressure within the Jandaíra formation itself did not play a significant role.

Building on models proposed by Roberts & Nunn (1995) and Sibson (2003), fracturing in low porosity rocks (the Jandaíra formation in our case) could be caused by increasing high pore pressures in an underlying permeable layer (the Açu sandstones). In contrast with these models, however, the evidence from the Jandaíra Formation shows that the fractures remained open and did not close until they were fully cemented. Possibly, stress levels in the Jandaíra formation remained high as a result of the stress concentration expected to take place in the rigid carbonates of the Jandaíra formation underlain by the softer Açu Sandstones (Lorenz *et al.*, 1991).

When deformation of the Jandaíra carbonates occurred, a network developed formed by mode I and hybrid fractures (Hancock, 1985). The hybrid nature of these fractures is documented by the evidence of shear along single veins and by the fact that the hybrid fractures are organised in conjugate patterns with a low inter-fault angle (Hancock, 1985).

In general, mechanic criteria to constrain the stress conditions at which hybrid fractures develop are missing (e.g. Engelder, 1999; Bertotti & Barnhoorn, 2016). According to Mohr-Coulomb diagram and theory, fractures with inter-fault angles of $<30^{O}$ can only be obtained with a tensional σ_3, which rarely exists in the Earth or with the help of high pore pressure (Secor, 1965; Hancock, 1985). Such an explanation is not applicable to the hybrid fractures of Jandaíra unit because (i) there was no porosity left inside the rock when fractures formed, and (ii) fractures remained mechanically open until they were cemented. This suggests that fluid pressures in the fractures were never substantially higher than hydrostatic values.

Hybrid fractures

Deformation in the carbonates of the Jandaíra Formation prior to the formation of sub-horizontal stylolites caused the development of two sets of structures, sub-vertical hybrid veins and stylolites. These features formed during subsidence and, therefore, should be common also in buried rocks which did not experience subsequent exhumation.

Hybrid veins and their occurrence in conjugate sets are rarely reported in the literature (e.g. Hancock, 1985; Belayneh & Cosgrove, 2010). We believe, however, that these features are not unique to the Jandaíra carbonates but have been overseen elsewhere because (i) joints and veins are often not analysed separately (see Peacock, 2004 for a similar comment), (ii) the insufficient attention paid to the sense of movement recorded in veins and (iii) the fact that small inter-fault angles such the ones we have measured are easily dismissed as resulting from measurement errors or not further specified natural variability.

Conjugate sets of hybrid fractures have been documented, for instance, from the Berda and Kef Eddour carbonate formation of Tunisia (Bisdom *et al.*, 2013). Here, sedimentary surfaces (pavements) steepened in association with the Alima anticline (e.g. Riley *et al.*, 2011; Said *et al.*, 2011) expose beautiful fracture networks composed of hybrid conjugate veins with shear documented by *en-echelon* gashes (Fig. 12) roughly perpendicular to bedding. The conjugate fractures have an intersection perpendicular to bedding and display dihedral angles <30°, comparable with those observed in the Jandaíra Formation. A few sub-vertical stylolites perpendicular to the trend of the conjugate faults could also be documented despite being sometimes overprinted by other structures developed during anticline folding (e.g. Bisdom *et al.*, 2013).

In the Triassic Latemar platform, a poorly clustered group of fractures is observed with a general NNW-SSE trend which was interpreted as resulting from one single strain episode (Boro, 2012; Boro *et al.*, 2013). Observation in single outcrops, however, documents the existence of two sets of fractures with an interfault angle of $\approx 20^{o}$ (Fig. 13a). These fractures are interpreted as coeval with the emplacement of 240–230 Ma old magmatic dykes and, therefore are thought to have formed during subsidence (Preto *et al.*, 2011; Boro, 2012; Boro *et al.*, 2013; Jacquemyn *et al.*, 2014). Similar to what documented for the Jandaíra carbonates, veins parallel to the fractures mentioned above are overprinted by bedding-parallel stylolites (Fig. 13b).

All in all, the structures observed in the Berda and Kef Eddour of Central Tunisia and in the Latemar carbonate platform closely recall the ones we have documented in the Jandaíra Formation, strengthening the hypothesis that syn-subsidence deformation leading to the development of bedding-perpendicular mode I, conjugate hybrid fractures and associated stylolites could be a common feature in buried rocks.

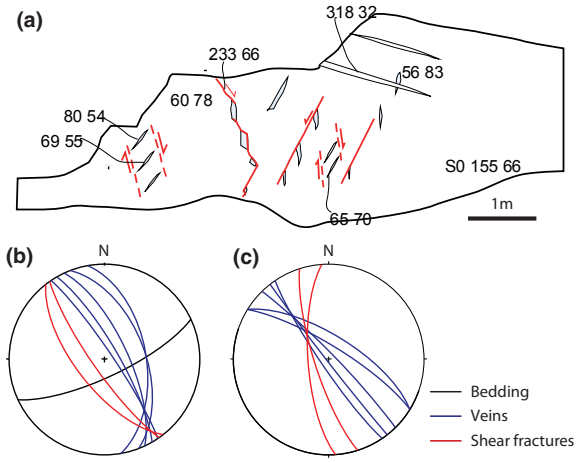

Fig. 12. Syn-subsidence deformation in the Upper Cretaceous Berda Formation (Central Tunisia); (a) Line drawing and stereoplot of outcrop TU4 (Selja gorge, Alima anticline). The surface shown in the drawing corresponds the lower bedding surface of a steeply SE dipping layer. The gently dipping veins visible in the upper part of the outcrop are associated with folding and not considered here. (b) stereoplot of the geometric elements shown in the line drawing; (c) geometric elements position of fractures and veins once bedding is rotated back to horizontal.

Fracture reactivation during exhumation

The wholesale deformation affecting the Jandaíra carbonate during subsidence caused the development of a pervasive system of well-clustered discontinuities which are likely to have impacted the originally isotropic character of the carbonates at least in the bedding-parallel dimension. To discuss the question of how the rock reacted to subsequent changes in stresses and, in particular, to exhumation, we compare the geometric properties of non-reactivated sub-vertical veins and stylolites with those of open (barren) fractures which, presumably formed/opened during Tertiary exhumation (Fig. 14).

The stereoplots of the non-reactivated veins and stylolites and that of the open fractures display remarkable similarities (Fig. 14) showing that few fractures were created during exhumation with directions different from those developed during subsidence. Spacing distances between preserved veins (Fig. 9) seem to be smaller than those between open fractures (Fig. 14) (0.75 m and 1–3 m respectively) suggesting that the barren fractures reactivated a large number but not all of the pre-existing veins. Our third observation is that open fractures are significantly longer than sub-vertical veins and stylolites (Figs 9 and 14). We interpret this observation as an indication that most of the deformation taking place during exhumation in the present stress field (Reis *et al.*, 2013) was accommodated by the reactivation and growth (increase in length) of a large portion of the discontinuities formed during subsidence.

It is worth noting that exhumation is a widespread phenomenon not only in rocks presently lying at or close to the surface, but also in those buried rocks which experienced episodes of upward movements in their geologic evolution followed by renewed subsidence. This is the case, for instance, of pre-Permian rocks underneath the Hercynian unconformity in North Africa (e.g. English *et al.*, 2016) and Mesozoic rocks underlying the Base Tertiary Unconformity in the North Sea. A comprehension of the full, multiphase structural evolution of these rocks is needed to provide meaningful predictions, for instance, of their fracture pattern.

Implications for reservoir studies

As most of the fractures and stylolites documented in the Jandaíra Fromation and elsewhere developed during subsidence, the results of our study bear important implications for the prediction of the characteristics and behaviour of reservoirs. Fractures and stylolites observed in the case studies mentioned above, formed in a fairly

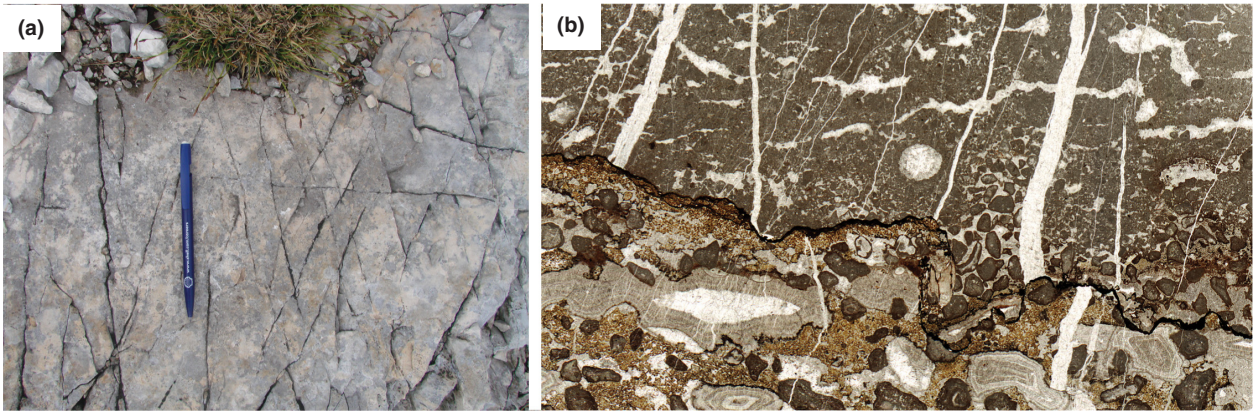

Fig. 13. Syn-subsidence deformation in the Middle Triassic Latemar platform (Dolomites, NE Italy) (a) conjugate veins with low inter-fault angle exposed on a small pavement. (b) thin section showing veins overprinted by sub-horizontal stylolites (photo courtesy by A. Immenhauser).

common tectonic setting characterised by the presence of a significant sub-horizontal stress of non-gravity origin. We therefore predict that they should be fairly ubiquitous subsurface features. In the case of the Kef Eddour and Berda Formations (Tunisia), this sub-horizontal stress further caused regional folding thereby underlying the importance of layer parallel shortening (e.g. Ahmadhadi *et al.*, 2008). High pore pressure in the carbonate prior to fracturing was low and did not play a significant role.

The fracture network was composed of mode I and hybrid fractures and, perpendicular to them, by stylolites. The first ones formed roughly parallel to the maximum compressional stress and remained open until they were cemented; stylolites, on the contrary, remained probably closed until the regional stresses changed. Resulting permeability was, therefore, strongly anisotropic.

A good knowledge of timing of fracture development is obviously key for the assessment of the petroleum system

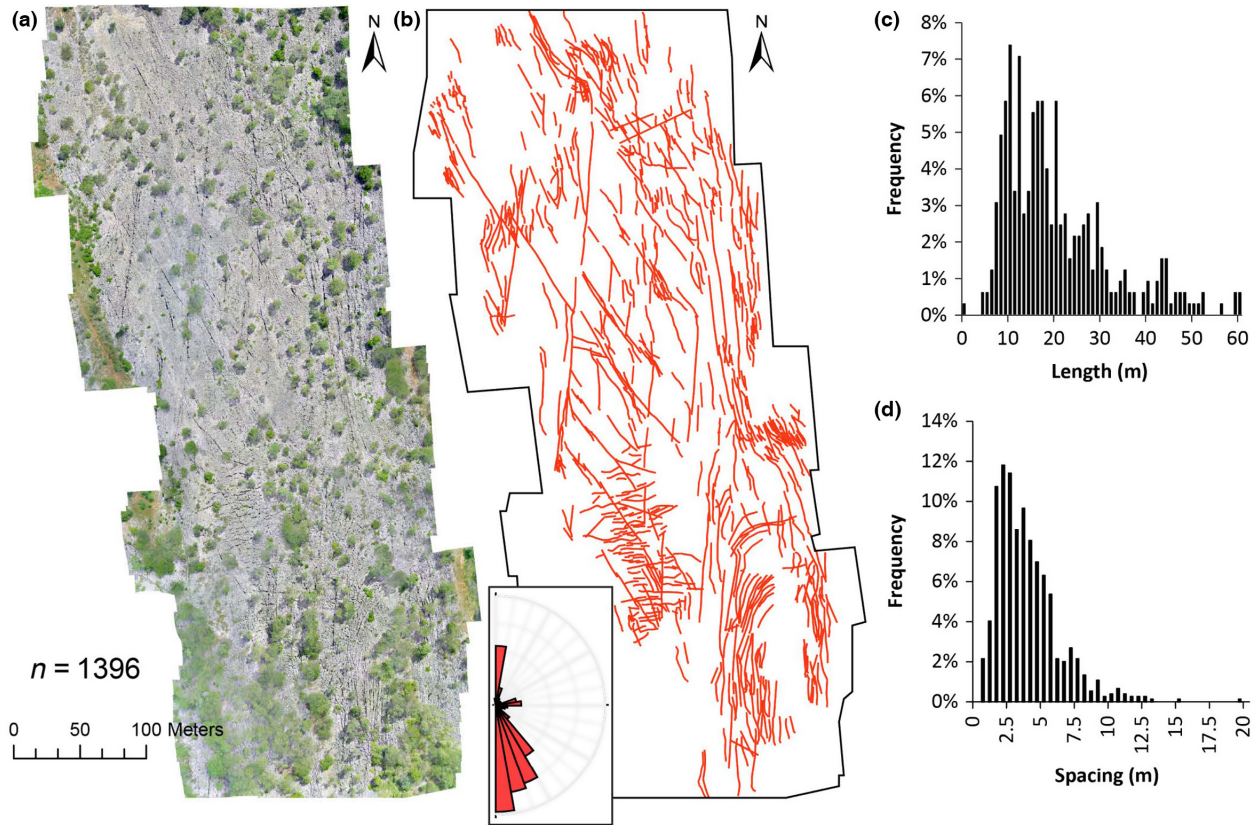

Fig. 14. The network of open fractures visible in outcrop AP3 of the Jandaíra carbonates. (a) high-resolution 2D outcrop model compiled from drone images; (b) map of the 1396 digitised lineaments (barren fractures and generally E-W reactivated stylolites; (c) length distribution of all barren fractures; (d) spacing distribution. Note how the directions of barren fractures are very similar to those of sub-vertical veins and stylolites shown in (Fig. 9).

and, in particular, for the quality of the potential seal. In the Potiguar basin, hydrocarbons were generated roughly between 110–100 and 50–60 Ma (Trindade *et al.*, 1992). Assuming a representative subsidence rate of a few centimeters per year, this is significantly younger then the time when the Jandaíra carbonates reached the depth at which sub-horizontal stylolites formed thereby sealing the pre-existing fracture system.

CONCLUSIONS

Shallow water carbonates of the Upper Cretaceous Jandaíra Formation, a post-rift succession of the Potiguar Basin presently outcropping in NE Brazil with very gentle dips to the NE and nearly devoid of large scale deformations, are affected by a pervasive network of sub-vertical veins, barren fractures and stylolites as well as sub-horizontal stylolites. The characteristics and position of these structures are fairly constant over tens of kilometres and are, therefore, associated with regional stresses and deformations.

Veins and stylolites formed during post-rift subsidence in a stress field characterised by the presence of a sub-horizontal stress probably of tectonic origin. We suggest that the dominant episode of deformation occurred when the presently outcropping rocks reached depths of 500–800 m and was accommodated by sub-vertical dm- to m-scale mode I to hybrid fractures oriented roughly N-S and by associated sub-vertical E-W trending stylolites. Hybrid fractures are organised in a conjugate pattern documenting the vertical position of the intermediate principal stress σ_2. As consequence of fracturing, the previously tight Jandaíra limestones acquired a fracture-related porosity thereby providing new pathways for fluid circulation. These pathways were used by meteoric fluids charged from the hinterland, mostly flowing along the underlying Açu Sandstones and eventually moving upward to the surface through the fractured Jandaíra carbonates.

With progressive subsidence, rocks entered a depth domain characterised by a sub-vertical maximum principal stress σ_1 which caused the formation of sub-horizontal stylolites. Calcite liberated by pressure solution precipitated in the open fractures sealing them and dramatically lowering the formation porosity and permeability.

During their exhumation to the surface, veins and stylolites in the presently outcropping portion of the Jandaíra Formation grew in length leading to the apparent networks visible in aerial images.

Sub-vertical fractures and stylolites as well as sub-horizontal stylolites, all formed during the subsidence phase of the Jandaíra Formation and are expected, therefore, to be present also in comparable rocks which did not experience exhumation. This should be the case, for instance, of the offshore part of the Potiguar basin where the Jandaíra carbonates are at depths >1–2 km and in other similar basins.

ACKNOWLEDGEMENTS

This contribution stems from the collaboration between UFRN, TUDelft and the VU University Amsterdam which benefitted from support by CNPq (Research Council of Brazil) and ANP (National Petroleum Agency of Brazil). We thank the numerous MSc students who participated in the project and colleagues and friends from UFRN (N. Srivastava, M. Videla among others) and from the Federal University of Campina Grande (C. Nogueira and A. Soares). Their contribution has been fundamental for the success of the project. The help and support of. Prof. S. Bouaziz (Sfax) for fieldwork in Tunisia is gratefully acknowledged.

CONFLICT OF INTEREST

No conflict of interest declared.

REFERENCES

Ahmadhadi, F., Daniel, J.M., Azzizadeh, M. & Lacombe, O. (2008) Evidence for pre-folding vein development in the Oligo-Miocene Asmari Formation in the Central Zagros Fold Belt, Iran. *Tectonics*, **27**. https://doi.org/10.1029/2006TC001978.

de Araripe, P.T. & Feijó, F.J. (1994) Bacia Potiguar. *Boletim de geociencias da petrobrás*, **8**, 127–141.

Belayneh, M. & Cosgrove, J.W. (2010) Hybrid veins from the southern margin of the Bristol Channel Basin, UK. *J. Struct. Geol.*, **32**, 192–201.

Bell, J.S. & Babcock, E.A. (1986) The stress regime of the western Canadian basin and implication for hydrocarbon production. *Bull. Can. Pet. Geol.*, **34**, 364–378.

Bertani, R.T., da Costa, I.G. & de Matos, R.M. (1990) Evolacao tectono-sedimentar, estilo estrutural, e habitat do petroleo na bacia Potiguar. In: *Origem e Evolucao de Bacias Sedimentares, Petrobras* (Ed. by G.P. Raja Gabagli & E.G. Milani), pp. 291–310. Petrobras, Rio de Janeiro.

Bertotti, G. & Barnhoorn, A. (2016) Geology of mode I, hybrid and mode II fractures: what do we really know? 78th EAGE Conference and Exhibition 2016, Vienna, 3, doi: 10.399/2214-4609.201601352

Bisdom, K., Bertotti, G., Gauthier, B.D.M. & Hardebol, N.J. (2013) A geologically consistent permeability model of fractured folded carbonate reservoirs: Lessons from outcropping analogue. 2nd EAGE Workshop on Naturally Fractured Reservoirs, 8-11 December 2013, Muscat, Oman, 1-6. https://doi.org/10.3997/2214-4609.20132006.

Bisdom, K., Bertotti, G. & Nick, H.M. (2016) The impact of different aperture distribution models and critical stress criteria on equivalent permeability in fractured rocks. *J. Geophys. Res. Solid Earth*. https://doi.org/10.1002/2015jb012657.

Bons, P.D., Elburg, M.A. & Gomez-Rivas, E. (2012) A review of the formation of tectonic veins and their microstructures. *J. Struct. Geol.*, **43**, 33–62.

Boro, H. (2012) Fracturing, Physical Properties and Flow Patterns in Isolated Carbonate Platforms: A field and numerical study of the Latemar Platform (Dolomites, N Italy). PhD Thesis Vrije Universiteit Amsterdam, 155 pp.

Boro, H., Bertotti, G. & Hardebol, N.J. (2013) Distributed fracturing affecting isolated carbonate platforms, the Latemar Platform Natural Laboratory (Dolomites, North Italy). *Mar. Pet. Geol.*, **40**, 69–84.

de Castro, D.L., Bezerra, F.H.R., Sousa, M.O.L. & Fuck, R.A. (2012) Influence of Neoproterozoic tectonic fabric on the origin of the Potiguar Basin, northeastern Brazil and its links with West Africa based on gravity and magnetic data. *J. Geodyn.*, **54**, 29–42.

Costa de Melo, A.C., de Castro, D.L., Rego Bezerra, F.H. & Bertotti, G. (2016) Rift fault geometry and evolution in the Cretaceous Potiguar Basin (NE Brazil) based on fault growth models. *J. South Am. Earth Sci.*, **71**, 96–107.

Couto Anjos, S.M., Sombra, C.L., de Souza, R.S. & Waick, R.N. (1990) Deep-Reservoir potential of Pendencia Formation, onshore Potiguar Basin. *Boletim Geociencias Petrobras*, **4** (4), 509–530.

Craig, H. (1961) Isotopic variations in meteoric waters. *Science*, **133**, 1702–1703.

Duhr, A. & Hilkert, A.W. & Thermo-Electron Corporation (2004) Finnigan GasBench II : δ 18 O and δ 13 C Determination of Carbonates, pp. 1–4.

Eberli, G.P., Baechle, G.T., Anselmetti, F.S. & Incze, M.L. (2003) Factors controlling elastic properties in carbonate sediments and rocks. *Lead. Edge*, **22**(7), 654.

Ebner, M., Koehn, D., Toussaint, R., Renard, F. & Schmittbuhl, J. (2009) Stress sensitivity of stylolite morphology. *Earth Planet. Sci. Lett.*, **277**(3–4), 394–398.

Engelder, T. (1999) Transitional-tensile fracture propagation: a status report. *J. Struct. Geol.*, **21**, 1049–1055.

English, J.M., English, K.L., Corcoran, D.V. & Toussaint, F. (2016) Exhumation charge : the last gasp of a petroleum source rock and implications for unconventional shale resources. *AAPG Bull.*, **100** (1), 1–16.

de Graaf, S., Bertotti, G., Reijmer, J., Bezerra, F.H.R., Cazarin, C.L., Bisdom, K. & Vonhoff, H. (2017) Fracture-controlled fluid circulation and calcite vein crystallization during early burial in shallow water carbonates (Jandaíra Formation, northeast Brazil). *Mar. Pet. Geol.*, **80**, 382–393.

Hancock, P.L. (1985) Brittle microtectonics: principles and practice. *J. Struct. Geol.*, **7**(3–4), 437–457.

Hardebol, N.H. & Bertotti, G. (2013) DigiFract: a software and data model implementation for flexible acquisition and processing of fracture data from outcrops. *Comp. Geosci.*, **54**, 326–336.

Heidbach, O., Tingay, M., Barth, A., Reinecker, J., Kurfeß, D. & Müller, B. (2010) Global crustal stress pattern based on the World Stress Map database release 2008. *Tectonophysics*, **482**(1–4), 3–15.

Hoefs, J. (1973) *Stable Isotope Geochemistry*, 142 pp. Springer, New York.

Hudson, J.D. (1977) Stable isotopes and limestone lithification. *Geol. Soc. Lond.*, **133**, 637–660.

Jacquemyn, C., el Desouky, H., Hunt, D., Casini, G. & Swennen, R. (2014) Dolomitization of the Latemar platform: fluid flow and dolomite evolution. *Mar. Pet. Geol.*, **55**, 43–67.

Javernick, L., Brasinton, J. & Caruso, B. (2014) Modeling the topography of shallow braided rivers using Structure-from-Motion photogrammetry. *Geomorphology*, **213**, 166–172.

Lamarche, J., Lavenu, A.P.C., Gauthier, B.D.M., Guglielmi, Y. & Jayet, O. (2012) Relationships between fracture patterns, geodynamics and mechanical stratigraphy in Carbonates (South-East Basin, France). *Tectonophysics*, **581**, 231–245.

Lorenz, J.C., Teufel, L.W. & Warpinski, N.R. (1991) Regional Fractures I: a mechanism for the formation of regional fractures at depth in flat-lying reservoirs. *Am. Assoc. Pet. Geol. Bull.*, **75** (11), 1714–1737.

Maraschin, A.J., Mizusaki, A.M.P., de Ros, L.F., The, S. & May, N. (2004) Northeastern Brazil Near-Surface K-feldspar precipitation in Cretaceous Sandstones from the Potiguar Basin, Northeastern Brazil. *J. Geol.*, **112** (3), 317–334.

de Matos, R.M.D. (1992) The Northeast Brazilian Rift System. *Tectonics*, **11** (4), 766.

Mello, U.T. (1989) Tectonic controls in the stratigraphy of the Potiguar Basin; An Integration of geodynamic models. *Buletim Geociencias Petrobras*, **3**(4), 347–364.

Morais-Neto, J.M., Hegarty, K.A., Karner, G.D. & Alkmim, F.F. (2009) Timing and mechanisms of generation and modification of of the anomalous topography of the Borborema Province, northeastern Brazil. *Mar. Pet. Geol.*, **26**, 1070–1086.

Nogueira, F.C.C., Marques, F.O., Bezerra, F.H.R., de Castro, D.L. & Fuck, R.A. (2015) Cretaceous intracontinental rifting and post-rift inversion in NE Brazil: Insights from the Rio do Peixe Basin. *Tectonophysics*, **644–645**, 92–107.

Olson, J.E. (2003) Sublinear scaling of fracture aperture versus length: an exception or the rule? *J. Geophys. Res.*, **108**(B9), 2413.

Pascal, C. & Cloetingh, S.A.P.L. (2009) Gravitational potential stresses and stress field of passive continental margins: insights from the south-Norway shelf. *Earth Planet. Sci. Lett.*, **277**(3–4), 464–473.

Peacock, D.C.P. (2004) Differences between veins and joints using the example of the Jurassic limestones of Somerset. *Geol. Soc. Lond. Spec. Publ.*, **231**(1), 209–221.

Preto, N., Franceschi, M., Gattolin, G., Massironi, M., Riva, A., Gramigna, P., Bertoldi, L. & Nardon, S. (2011) The Latemar: a Middle Triassic polygonal fault-block platform controlled by synsedimentary tectonics. *Sed. Geol.*, **234** (1–4), 1–18.

Reis, Á.F.C., Bezerra, F.H.R., Ferreira, J.M., do Nascimento, A.F. & Lima, C.C. (2013) Stress magnitude and orientation in the Potiguar Basin, Brazil: implications on faulting style and reactivation. *J. Geophys. Res. Solid Earth*, **118** (10), 5550–5563.

Riley, P., Gordon, C., Simo, J.A., Tikoff, B. & Soussi, M. (2011) Structure of the Alima and associated anticlines in the foreland basin of the southern Atlas Mountains, Tunisia. *Lithosphere*, **3**(1), 76–91.

Roberts, S.J. & Nunn, J.A. (1995) Episodic fluid expulsion from geopressured sediments. *Mar. Pet. Geol.*, **12**, 195–204.

Said, A., Baby, P., Chardon, D. & Ouali, J. (2011) Structure, paleogeographic inheritance, and deformation history of the Southern Atlas foreland fold and thrust belt of Tunisia. *Tectonics*, **30**(6), 1–15.

Sanderson, D.J. & Nixon, C.W. (2015) The use of topology in fracture network characterization. *J. Struct. Geol.*, **72**(55), 66.

Schmittbuhl, J., Renard, F., Gratier, J.-P. & Toussaint, R. (2004) Roughness of stylolites: implications of 3D high resolution topography measurements. *Phys. Rev. Lett.*, **93**(23), 238501.

Secor, D.T. (1965) Role of fluid pressure in jointing. *Am. J. Sci.*, **263**, 633–646.

Sibson, R.H. (2000) Fluid involvement in normal faulting. *J. Geodyn.*, **29**(3–5), 469–499.

Sibson, R.H. (2003) Brittle-failure controls on maximum sustainable overpressure in different tectonic regimes. *AAPG Bull.*, **87**(6), 901–908.

Snow, D.T. (1969) Anisotropic permeability of fractured media. *Water Resour. Res.*, **5**(6), 12–73.

Tavani, S., Granado, P., Corradetti, A., Girundo, M., Iannace, A., Arbués, P., Muñoz, J.A. & Mazzoli, S. (2014) Building a virtual outcrop, extracting geological information from it, and sharing the results in Google Earth via OpenPlot and Photoscan: an example from the Khaviz Anticline (Iran). *Comput. Geosci.*, **63**, 44–53.

Tibana, P. & Terra, G.J.S. (1981) Sequencias carbonaticas do Cretaceo na bacia Potiguar. *Boletim tecnico Petrobras*, **24**(3), 174–182.

Trindade, L.A.F., Brassell, S.C. & Santos Neto, E.V. (1992) Petroleum Migration and Mixing in the Potiguar Basin, Brazil. *AAPG Bull.*, **76**(12), 1903–1924.

Vonhof, H.B., Breukelen, M.R., Postma, O., Rowe, P.J., Atkinson, T.C. & Kroon, D. (2006) A continuous-flow crushing device for on-line d2H analysis of fluid inclusion water in speleothems. *Rapid Commun. Mass Spectrom.*, **20**, 2553–2558.

Zoback, M. (2007) *Reservoir Geomechanics*. Cambridge University Press, Cambridge, UK.

Manuscript received 10 August 2016; In revised form 31 March 2017; Manuscript accepted 6 April 2017.